

Article

Elimination of the Inrush Current Phenomenon Associated with Single-Phase Offline UPS Systems

Syed Sabir Hussain Bukhari, Shahid Atiq and Byung-il Kwon *

Department of Electronic Systems Engineering, Hanyang University ERICA, Ansan 426-791, Korea; sabir@hanyang.ac.kr (S.S.H.B.); shahidatiq@hanyang.ac.kr (S.A.)

* Correspondence: bikwon@hanyang.ac.kr; Tel.: +82-31-400-5165

Academic Editor: Gabriele Grandi

Received: 4 December 2015; Accepted: 28 January 2016; Published: 4 February 2016

Abstract: Critical load applications always rely on UPS systems to uphold continuous power during abnormal grid conditions. In case of any power disruption, an offline UPS system starts powering the load to avoid blackout. However, this process can root the momentous inrush current for the transformer installed before the load. The consequences of inrush current can be the reduction of output voltage and tripping of protective devices of the UPS system. Furthermore, it can also damage the sensitive load and decrease the transformer's lifetime. To prevent the inrush current, and to avoid its disruptive effects, this research suggests an offline UPS system based on a current regulated inverter that eliminates the inrush current while powering the transformer coupled loads. A detailed comparative analysis of the conventional and proposed topologies is presented and the experiment was performed by using a small prototype to validate the performance, and operation of the proposed topology.

Keywords: uninterruptible power supply; offline; inrush currents; current regulation

1. Introduction

The stability of power is a key concern for domestic, commercial, and industrial users these days. Sags, swells, and outages over and over again interrupt the operational processes, and even lead to equipment impairment [1,2]. Intended for the continuous operation of critical loads, such as flexible speed drives, semiconductor processing tools, and industrial, commercial, and life-supporting systems, a UPS system is usually installed to keep the power during any abnormal grid condition [2–5]. These UPS systems can be categorized into different types based on their configuration and operating principles. However, this paper focuses on the single-phase topology of an offline UPS system.

An offline UPS topology is sometimes named as line-preferred and involves of a main switch to connect the load directly to the utility, a battery that can be charged using a charger/rectifier, an inverter to power the load from the battery during abnormal grid conditions, and an alternate switch to connect the load to the UPS system [6]. The power rating of the charger is about 20% and the inverter is about 100%, hence the overall power capacity of this topology is about 120% of the output power [7]. The major advantages of an offline UPS system are; high efficiency, small size, simple design, and low cost. In addition to the several advantages, some of the negatives associated with this topology are the absence of isolation for critical loads and the power provided to the load is not controlled, hence the load is not guarded from any of the transient occurrence at the utility side [3,8]. Due to this reason, a single-phase offline UPS topology is used for low power applications. To overcome this issue and to provide isolation for the load, a load transformer is generally installed between the load and the utility. Additional disadvantages include the performance issues with the nonlinear loads [6] and the larger load transfer switching time interval [8]. During this interval, a flux offset

is established for the load transformer which was installed before, for electrical isolation or voltage matching purposes. Hence, as soon as the UPS reinstates the load voltage, the transformer flux may increase beyond its threshold and causes magnetic saturation. This saturation of the load transformer generates the serious magnitude of inrush current [1,9]. The magnitude of this inrush current may increase from two to six times the load current. However, it depends on various factors including the voltage injection instant of the inverter and the properties of the load transformer [10]. The inrush current decreases the output voltage, actuate the protection devices of the system, and damage the sensitive load. Furthermore, it can also damage the transformer and decrease its lifetime [9,11,12].

Many solutions which were previously used for the transformer inrush current mitigation, can also be used for an offline UPS system powering a transformer-coupled sensitive load. However, most of them have some disrupting effects on the UPS topology on the cost of inrush current mitigation for example, by decreasing the voltage during the generation of inrush current or by turning on the inverter voltage at the proper phase angle can reduce the inrush current phenomenon [13,14] but it can cause an interruption for a longer time than the conventional single-phase offline UPS topology [1,15]. Introducing the resistors or reactors during the starting time of the UPS system can reduce the inrush current magnitude as well, but to accommodate these resistors, reactors, and electromechanical switches, a large power distribution panel is required [16]. Increasing the size of the load transformer at more than the rated flux density can also be an effective solution to deal with the inrush current issue, but it will increase the overall size and the cost of the system. A flux offset compensation method to regulate the flux of the transformer may also be used. However, it complicates the implemented control algorithm for the UPS system [1,17].

Headed for the elimination of inrush current associated with a single-phase offline UPS system during the transfer of load, this paper proposes a new single-phase offline UPS topology that utilizes a current regulating scheme for the inverter implemented in a stationary frame of reference. This current control strategy is based on recently-established high-bandwidth control strategies which are originally designed for motor controls [2]. However, these algorithms are also applicable for regulating AC currents for any balanced load [18]. Adding to the complete elimination of inrush current, this control strategy enables the proposed offline UPS system to offer better performance while dealing with nonlinear loads. Since the probability of the inrush current is completely eliminated and the isolation for the load is achieved without any risk, hence the proposed offline UPS system may be employed for higher power use.

2. Basic Operating Principle

The operational principles of the conventional and proposed single-phase offline UPS systems are discussed below:

2.1. Conventional Single-Phase Offline UPS System

Figure 1a shows a basic diagram of an offline UPS system. During the normal utility power condition the inverter is bypassed by the main switch (S_M) and the load is delivered power directly by the utility without any isolation. Throughout this operation, the system is said to be in normal mode. Meanwhile, the battery is charged by the charger/rectifier and the inverter remains off. However, when the utility experiences any fault, the main switch (S_M) opens to isolate the load from the utility and the alternate switch (S_A) energizes to supply the backup power of the battery. The system is said to be in inverter mode. This transition of load takes about 4 ms in most of the cases and can be as much as 20 ms depending on the fault detection and the load transition mechanisms [8]. The load transition time interval does not affect the loads without the load transformer and the load current remains the same, as seen in Figure 1b,c shows the load voltage under such condition.

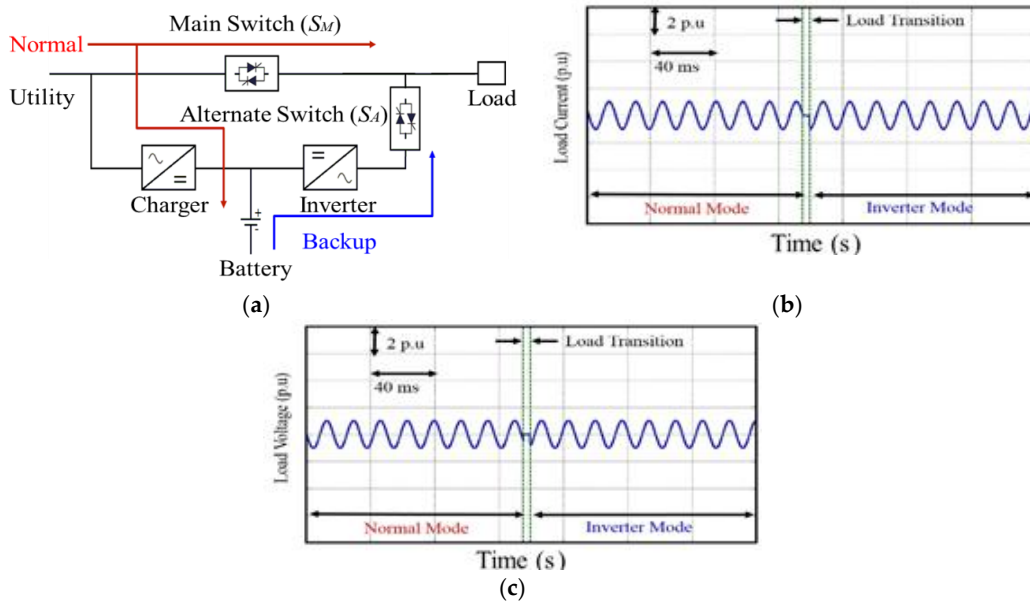


Figure 1. (a) Basic diagram of a single-phase offline UPS system without load transformer; (b) load current; and (c) load voltage.

For the acceptable isolation of load from the utility, a load transformer is generally installed before the load as shown in Figure 2a. The transition time interval, which did not affect the load current before *i.e.*, in case of load without the load transformer, can generate serious magnitude of inrush transient current during the starting of the UPS system while powering the transformer-coupled load. Figure 2b,c shows the behavior of an offline UPS system during such circumstances. From the figure, it is evident that the load current reaches to 5.54 per unit (p.u) which is more than five and a half times higher than the rated steady-state magnitude. Figure 3a,b shows the flowcharts for a typical offline UPS system to illustrate the transfer of load from normal operating to the inverter modes, and *vice versa*.

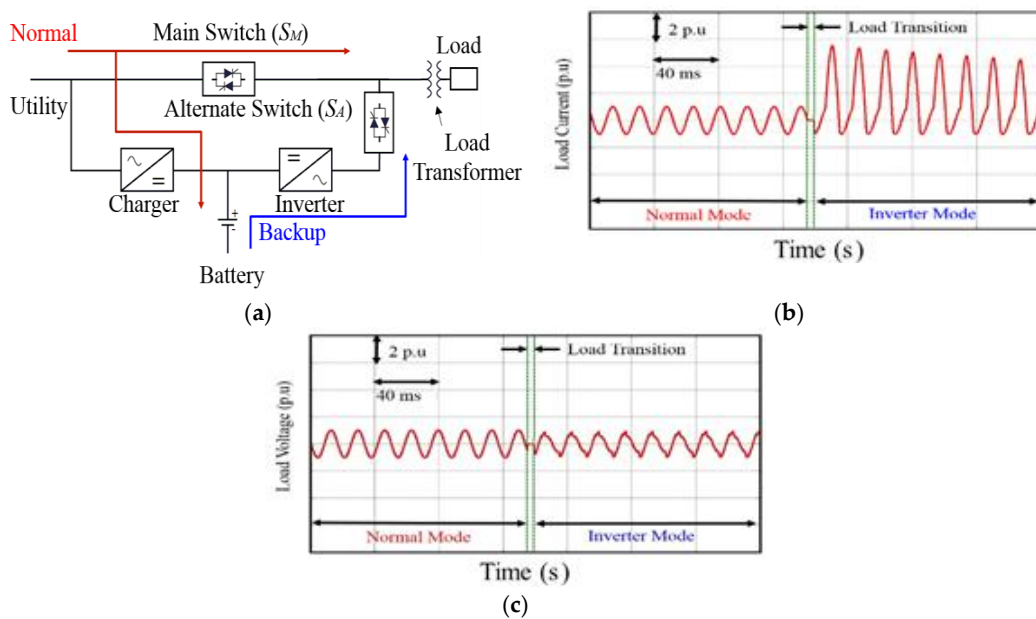


Figure 2. (a) Basic diagram of a single-phase offline UPS system with load transformer; (b) load current; and (c) load voltage.

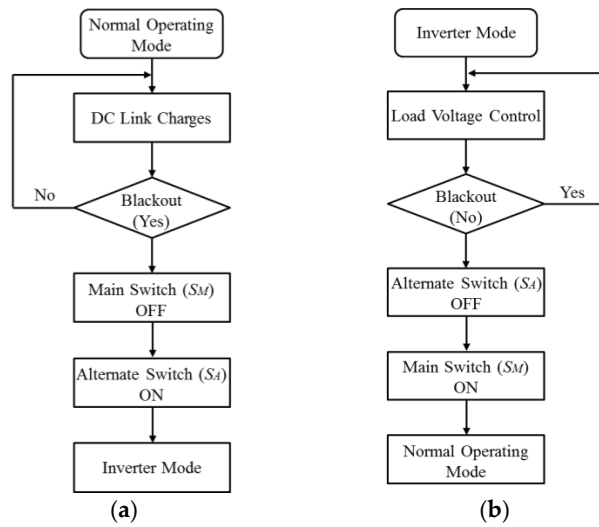


Figure 3. Flowchart for the (a) normal operating; and (b) inverter modes of the conventional offline UPS system.

2.2. Proposed Single-Phase Offline UPS System

To eliminate the inrush current for an offline UPS system when it is powering the load transformer, this paper offers an offline UPS topology based on a current regulated inverter instead of the conventional PWM voltage source inverter. Basic operational principle of the suggested UPS system is similar as the conventional topology shown in Figures 1a and 2a. However, the risk of inrush current is rejected by using a current control algorithm implemented in a stationary frame of reference. Figure 4a,b shows the complete illustration of the proposed topology along with the filter circuit. As shown in Figure 4b, the filter circuit consists of an inductor and a capacitor connected in parallel to each other to remove the current and voltage ripples of the inverter, respectively.

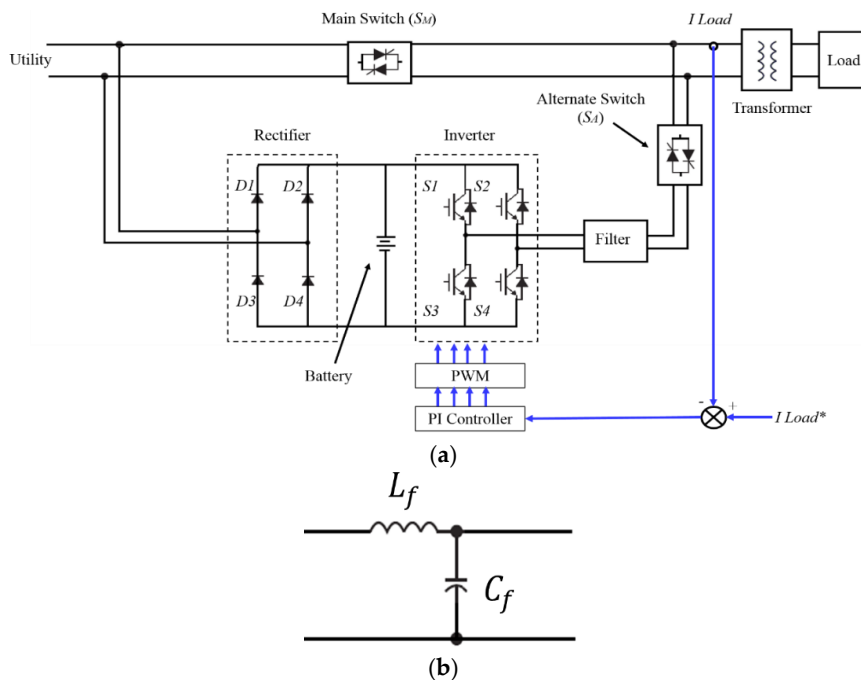


Figure 4. (a) Complete diagram of the proposed single-phase UPS system with load transformer; and (b) filter circuit.

The current-regulating algorithm employed for the proposed UPS system uses an improved current control scheme which is ideally suited for controlling AC currents with and without motor loads through a PI controller, as illustrated in [19]. Simplicity and ease in implementation are the only reasons for using this current control algorithm. Furthermore, a detailed analysis of the implemented current control strategy along its performance and stability issues are well discussed in [19]. However, any of the recently well-developed current regulating schemes can also be used for this purpose. The transfer function of the proposed system powering a load without associated EMF *i.e.*, RL load is given by:

$$I(s) = \frac{I^*(s) * G_c(s) * V_{DC} * G_p(s) * F(s)}{1 + G_c(s) * V_{DC} * G_p(s) * F(s)} \quad (1)$$

However, if the proposed UPS system is powering a motor load, same transfer function can be written as:

$$I(s) = \frac{I^*(s) * G_c(s) * V_{DC} * G_p(s) * F(s) - G_p(s) * D(s)}{1 + G_c(s) * V_{DC} * G_p(s) * F(s)} \quad (2)$$

where $I^*(s)$ is the reference command, $I(s)$ is the inverter output *i.e.*, measured load current, a linear amplifier with a forward gain of V_{DC} is used for the replacement of PWM modulator, $G_c(s)$ and $G_p(s)$ are the transfer functions of controller and plant, respectively, and the motor load's back EMF is modeled as a disturbance injection $D(s)$ using simple control theory [19]. However, $F(s)$ is the transfer function of the filter and is given by:

$$F(s) = \frac{1}{1 + s * L_f + s^2 * L_f * C_f} \quad (3)$$

where L_f is the filter inductance and C_f is the filter capacitance, respectively.

The function of the PI controller in the system is to equate the load current to the reference command as diligently as possible while minimizing any error caused by the disturbance injection $D(s)$. The transfer function of the plant is given by:

$$G_p(s) = \frac{1}{R(1 + sT)}, \quad T = \frac{L}{R} \quad (4)$$

$G_c(s)$ is given by:

$$G_c(s) = K_p \left[1 + \frac{1}{s\tau_r} \right] \quad (5)$$

where τ_r is the integrator reset time and is the ratio of proportional and integral gain (K_p/K_i).

By substituting from Equations (4) and (5), the open loop forward path gain of this system is obtained as:

$$G_p G_c(s) = \frac{V_{DC} * K_p * (1 + s\tau_r)}{R * \tau_r * s * (1 + sT)} \quad (6)$$

The operation of any control system is always influenced by two delays: (1) transport delay due to the PWM process and (2) sampling delay due to the digital control system. The total transport and sampling delay for the implemented current-regulating algorithm is about 0.75 [20] of the carrier period. The PWM carrier period in this case is about 100 μ s.

The control loop delays can be modeled by using Z-transform theory as discussed in [21] with a zero-order-hold element to model sampling delay and a $1/Z$ block in series with the controller to model transport delay. The average-value model diagram representations of the inverter with the properties of sampling and transport delays while powering an RL and motor loads are shown in Figure 5a,b. Figure 6 shows a Bode plot of Open Loop Forward Gain of the implemented current control algorithm, while considering transport and sampling delays. These plots are obtained under the conditions of passive RL load having $R = 90 \Omega$ and $L = 10$ mH, proportional gain $K_p = 5$ and integral gain $K_i = 0.5$, and total transport and sampling delays = 75 μ s [18–20]. From the figure it can be observed exactly

that how the controller delays cause the system phase to now roll off past the -180° stability limit at high frequency. This makes the maximum value of K_p to a value that keeps the system phase response less than -180° (i.e., a positive phase margin) at the unity gain crossover frequency. Figure 7 shows a comparative analysis of the experimental response of the implemented current regulator against the reference current. This figure shows that the response delay of the controller of the proposed UPS system obtained experimentally has insignificant magnitude and phase difference compared to the reference current [22]. Figure 8a,b shows the flowcharts to explain the transition of load from normal operating to the inverter modes and from inverter to the normal operating modes of the proposed topology. As seen from the flowchart, the process of transition of load for the proposed UPS system is similar to that of conventional offline UPS topology except of the controller, as the proposed topology utilizes current control strategy however, the conventional topology work on voltage control algorithm.

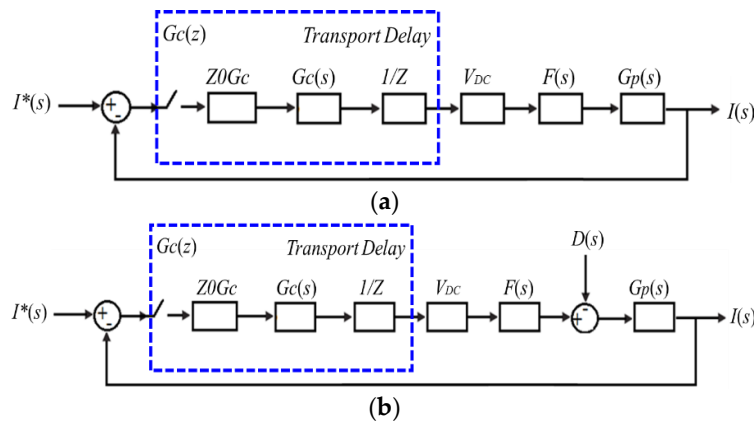


Figure 5. Average value diagram for the proposed system powering (a) RL load; and (b) motor load.

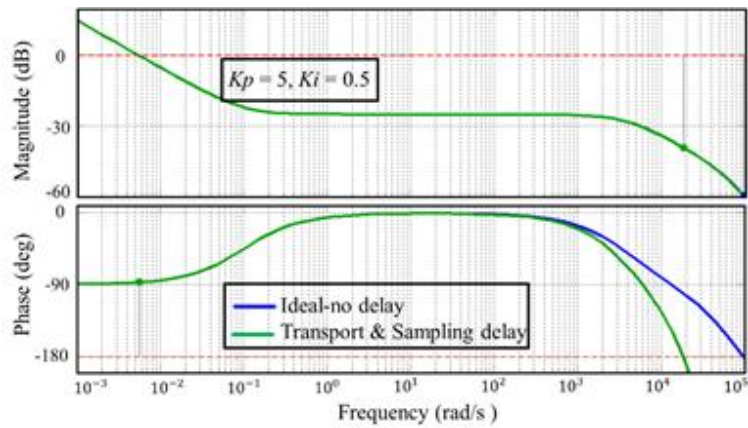


Figure 6. Bode plot of Open Loop Forward Path Gain for implemented controller.

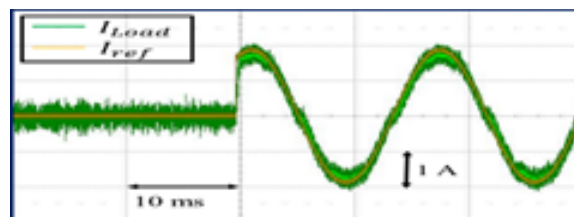


Figure 7. Experimental response of the current regulator implemented for the proposed system.

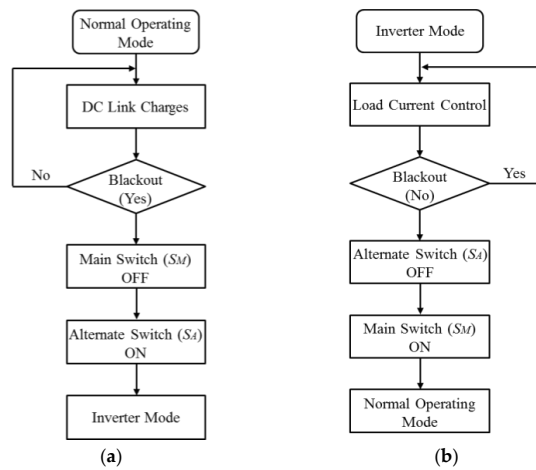


Figure 8. Flowchart for the (a) normal operating; and (b) inverter modes of the proposed system.

The reference current signal $I^*(s)$ can be generated by using a voltage loop outside the current loop. Under such condition the voltage error sets the current command for the inner loop via controller. The outer loop controls the load voltage by changing the reference of inner loop [23]. The inner loop controls the load current as discussed above. This enables the proposed single-phase UPS system to operate on flexible loading conditions. The average-value model diagram representation for the outer voltage loop of the proposed system is shown in Figure 9 and the transfer function is given by:

$$V(s) = \left[\frac{I^*(s) * G_c(s) * V_{DC} * G_p(s) * F(s)}{1 + G_c(s) * V_{DC} * G_p(s) * F(s)} \right] \cdot [G_{PV}(s) * Z(s) * V^*(s)] \quad (7)$$

The performance of the proposed system is shown in Figure 10, which suggests that the load current remains same as the case when the conventional offline UPS system was powering the load without the load transformer. The load current never exceeds 1 (p.u) at any stage during the load transition from the utility to the inverter. The load current and voltage is shown in Figure 10a,b, respectively. Furthermore, the proposed UPS system offers the similar advantages of simple design, and high efficiency as that of conventional single-phase topology. The size, weight, and cost of the proposed topology is comparatively greater than the conventional topology since it employs a load transformer for isolation purpose. A detailed comparison of both (proposed and conventional topologies) is given in Table 1.

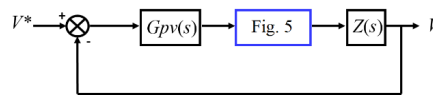


Figure 9. Average value model of the outer voltage loop of the proposed system.

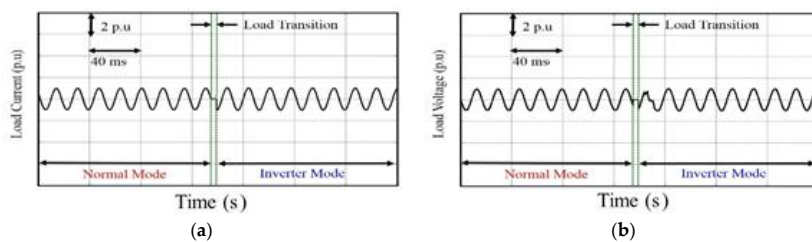


Figure 10. (a) Load current; and (b) load voltage of the proposed offline UPS system.

Table 1. Comparison of conventional and proposed offline UPS topologies.

Attribute	Conventional Topology	Proposed Topology
Power Application	Low Power Applications	Low-Medium Power Applications
Power Capacity	120%	120%
Efficiency	High	High
Design	Simple	Simple
Isolation of Load	No	Best
Cost, Size and Weight	Low	High (due to load transformer)
Inrush Current Possibility	Yes	No
Issues with Non-Linear loads	Yes	No

2.3. Inrush Current Phenomenon and Comparative Transient Behavior of the Conventional and Proposed Single-Phase Offline UPS Topologies

For the quantitative analysis of the inrush current phenomenon associated with a single-phase offline UPS system while powering a load transformer, consider the source voltage applied to the transformer is:

$$v = v_m \sin(\omega t + \alpha) \quad (8)$$

The resultant flux under steady-state operation is:

$$\varphi(t = 0) = -\varphi_m \cos(\omega t + \alpha) \quad (9)$$

When $t = 0$, the flux is:

$$\varphi_0 = -\varphi_m \cos(\alpha) \quad (10)$$

The initial value of the transient flux is equal in magnitude and opposite in sign to that given in following equation:

$$\varphi_t(t = 0) = \varphi_m \cos(\alpha) \quad (11)$$

Subscript t indicates the transient flux.

The instantaneous flux (λ) at any time t , is:

$$\lambda = \varphi_m [\cos(\alpha) - \cos(\omega t + \alpha)] \quad (12)$$

where $t \geq 0$.

To define the mechanism of generation of inrush current during the change of load from the utility to the inverter consider the following equation:

$$v = \frac{d\lambda}{dt} \quad (13)$$

where λ is the instantaneous flux and v is the voltage drop at the primary side of the load transformer.

The above equation suggests that the derivative of instantaneous flux with respect to time is proportional to the instantaneous voltage drop at the primary side of the transformer. For a load transformer, voltage, and flux waveforms are shifted by 90° during normal operation. However, during the transition of load these waveforms act differently. As the transition occurs and inverter restores the load voltage, the magnetic flux of the transformer increases above the normal operating value. Since the magnetization curve is nonlinear, this magnitude of flux causes the saturation of the load transformer. Under such a condition, high magnitude of MMF is necessary to cause flux. Hence, the current, that produces the MMF to root flux, will excessively increase beyond its normal peak. For the magnitude of the first cycle of inrush transient current, consider the following equation:

$$I_{peak} = \frac{\sqrt{2} * V_m}{\sqrt{(\omega * L)^2 + R^2}} \left(\frac{2 * B_n + B_r - B_s}{B_n} \right) \quad (14)$$

where L is the air core inductance, R is the total DC resistance, B_n , B_r , and B_s are the rated, remanent, and saturation flux densities of the transformer and V_m is the maximum applied voltage [24–26].

Equations (13) and (14) suggest that the magnitude of inrush current depends on the parameters *i.e.*, impedances of windings and the switching instant of the load transformer at which inverter injects the load voltages. To investigate the effect of winding impedances on the magnitude of inrush current study have been performed using four load transformers (T_1 , T_2 , T_3 , and T_4) with different impedances. The parameters of these investigated transformers are given in the following Table 2:

Table 2. Parameters of investigated load transformers.

Transformer	T ₁	T ₂	T ₃	T ₄
Rating (kVA)	1	1	1	1
Voltage	220	220	220	220
Turn Ratio	1:1	1:1	1:1	1:1
R_1 (Ω)	1.535	1.180	0.908	0.698
R_2 (Ω)	0.511	0.393	0.302	0.232
L_1 (mH)	2.059	1.584	1.218	0.937
L_2 (mH)	0.686	0.527	0.406	0.312

R_1 and L_1 is the resistance and inductance of the primary winding, and R_2 , and L_2 is the resistance and inductance of the secondary winding of the investigated load transformers.

Table 3 shows the magnitude of first, second, and third peaks of inrush current when the load transformers with the above parameters are used. The operating conditions for all load transformers are same in order for a more accurate comparison. From the results it is observed that as the impedances of the load transformer increases, the magnitude of inrush current decreases. Furthermore, increase in the impedances also fastens the decay process of inrush current.

Table 3. Comparison of maximum inrush current for different load transformers.

Transformer	First Peak (p.u)	Second Peak (p.u)	Third Peak (p.u)
T ₁	2.886	2.761	2.659
T ₂	2.911	2.811	2.730
T ₃	2.937	2.851	2.788
T ₄	2.973	2.897	2.834

To study the performance of the conventional and proposed offline UPS systems, investigations have been carried out over the wide range of switching instants for the load transformer when the inverter injects the load voltage shown in Figure 11. Figures 12a–24a show the load currents. However, the load voltages are shown in Figures 12b–24b. Transformer with the largest inrush current magnitudes shown in Table 3. *i.e.*, T_4 is used for this purpose. From the results it is evident that the magnitude of inrush current using the conventional offline UPS topology is different at different switching instants and it attains the maximum value when the inverter injects the load voltage at an angle of 330° . However, the load current for the proposed single-phase UPS system remains the same regardless the switching conditions. It never exceeds the prescribed value at any point as the transition of load from utility to the inverter occurs.

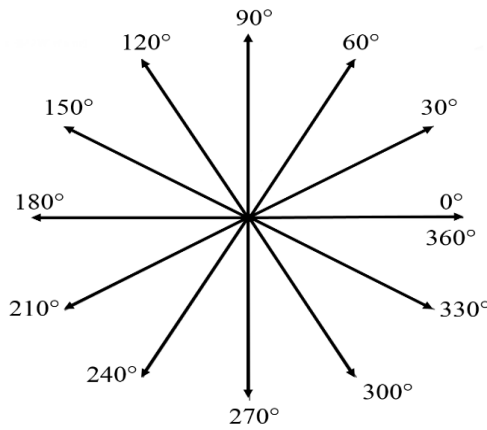


Figure 11. Switching conditions for the load transformer.

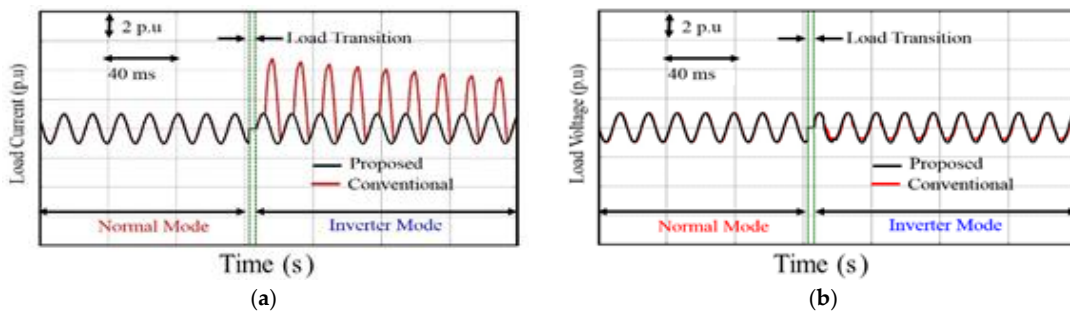


Figure 12. (a) Load current; and (b) load voltage for the conventional and proposed single-phase offline UPS topologies when the inverter voltage is injected at 0° .

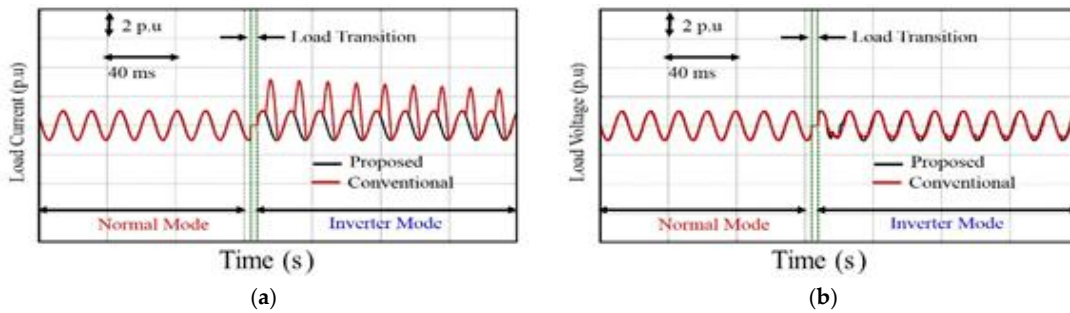


Figure 13. (a) Load current; and (b) load voltage for the conventional and proposed single-phase offline UPS topologies when the inverter voltage is injected at 30° .

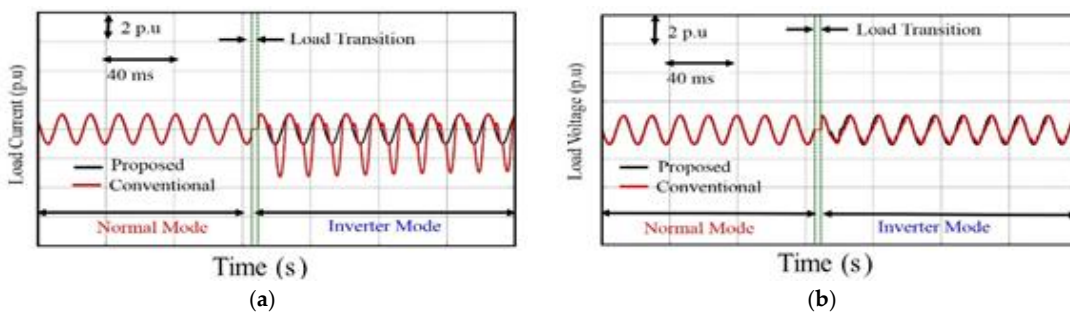


Figure 14. (a) Load current; and (b) load voltage for the conventional and proposed single-phase offline UPS topologies when the inverter voltage is injected at 60° .

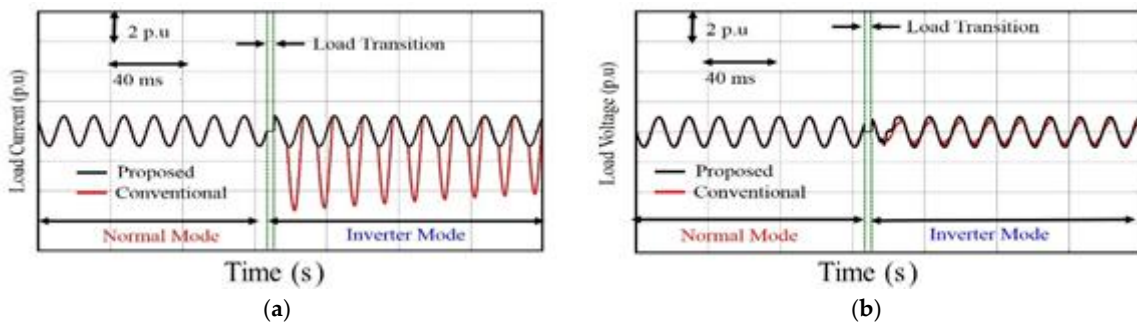


Figure 15. (a) Load current; and (b) load voltage for the conventional and proposed single-phase offline UPS topologies when the inverter voltage is injected at 90° .

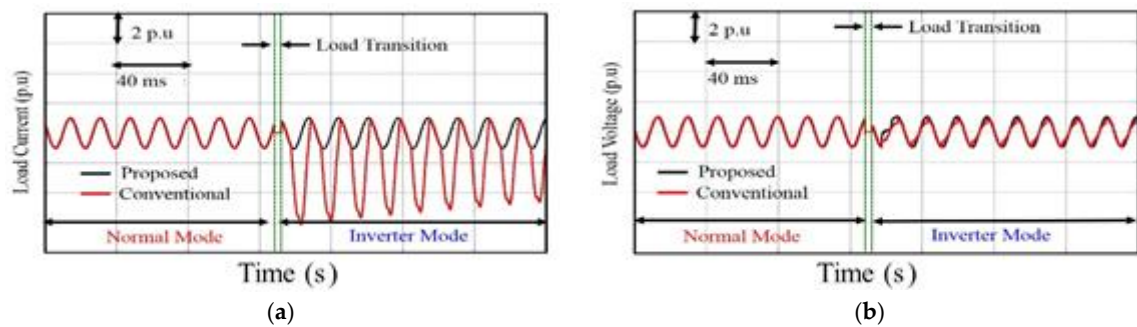


Figure 16. (a) Load current; and (b) load voltage for the conventional and proposed single-phase offline UPS topologies when the inverter voltage is injected at 120° .

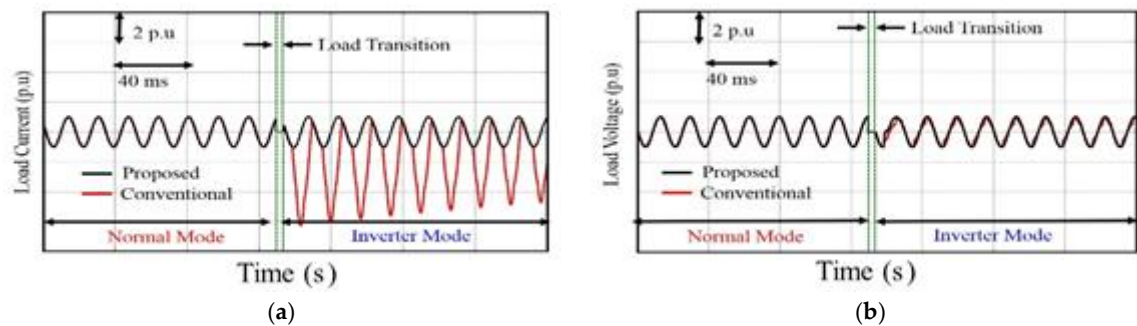


Figure 17. (a) Load current; and (b) load voltage for the conventional and proposed single-phase offline UPS topologies when the inverter voltage is injected at 150° .

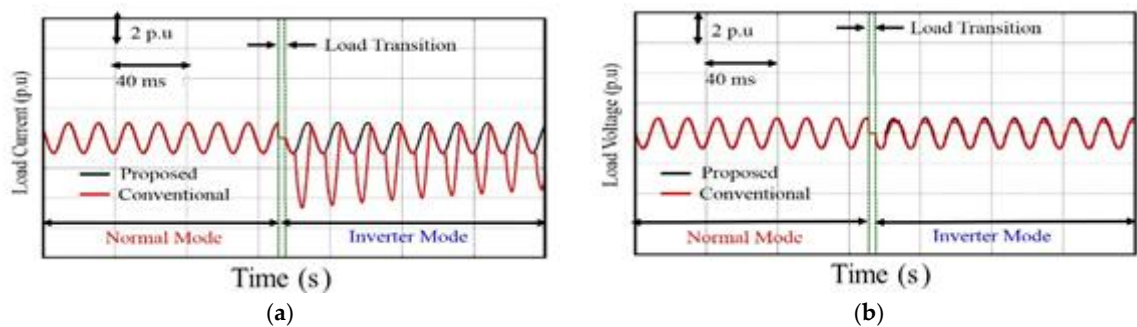


Figure 18. (a) Load current; and (b) load voltage for the conventional and proposed single-phase offline UPS topologies when the inverter voltage is injected at 180° .

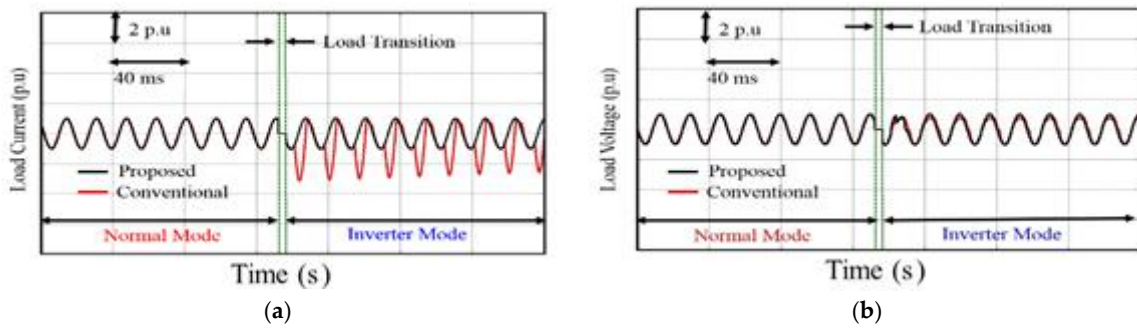


Figure 19. (a) Load current; and (b) load voltage for the conventional and proposed single-phase offline UPS topologies when the inverter voltage is injected at 210° .

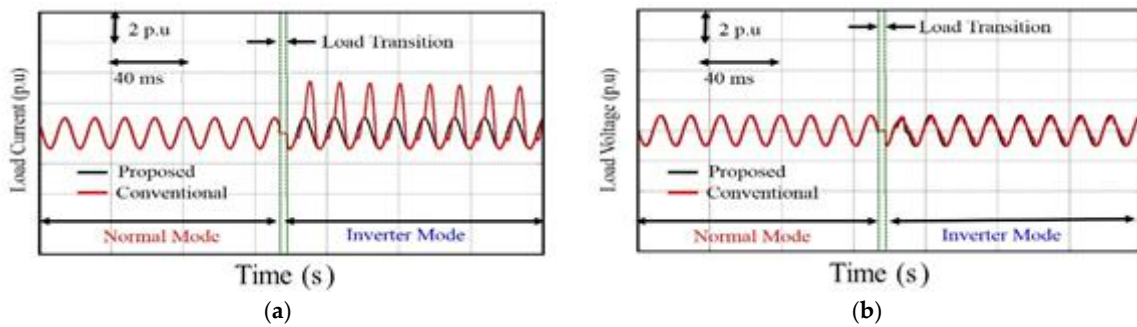


Figure 20. (a) Load current; and (b) load voltage for the conventional and proposed single-phase offline UPS topologies when the inverter voltage is injected at 240° .

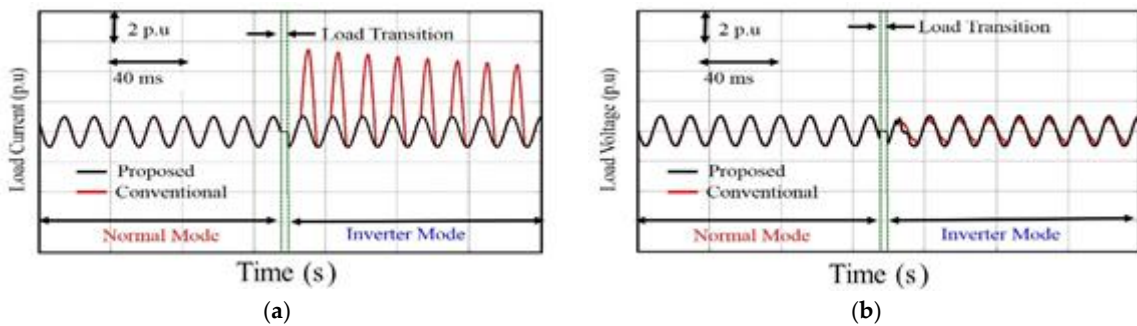


Figure 21. (a) Load current; and (b) load voltage for the conventional and proposed single-phase offline UPS topologies when the inverter voltage is injected at 270° .

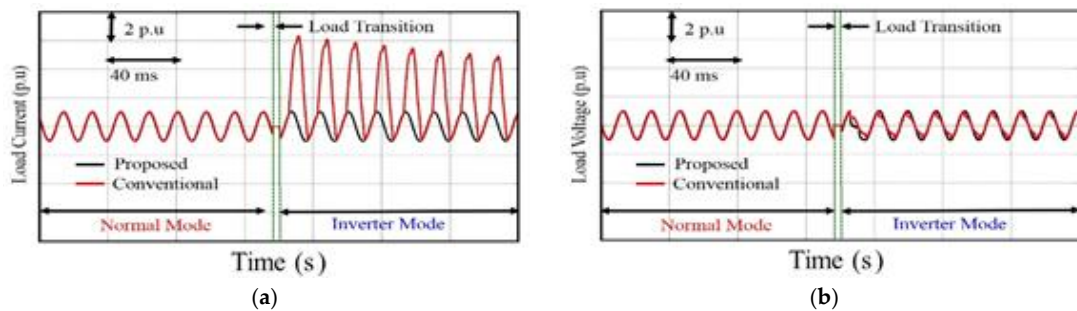


Figure 22. (a) Load current; and (b) load voltage for the conventional and proposed single-phase offline UPS topologies when the inverter voltage is injected at 300° .

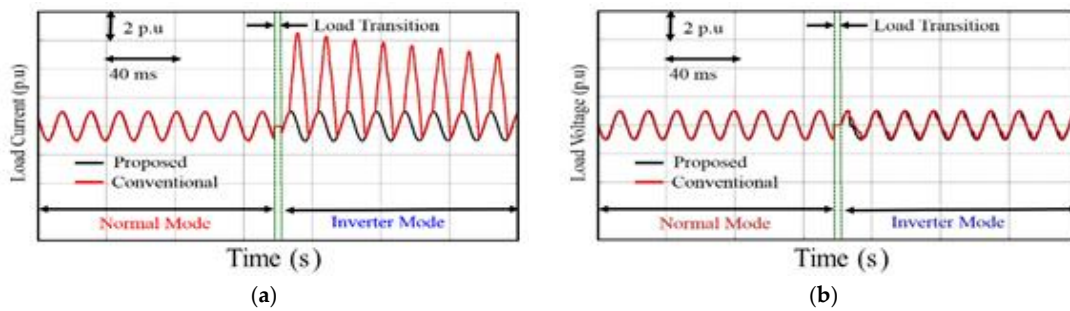


Figure 23. (a) Load current; and (b) load voltage for the conventional and proposed single-phase offline UPS topologies when the inverter voltage is injected at 330° .

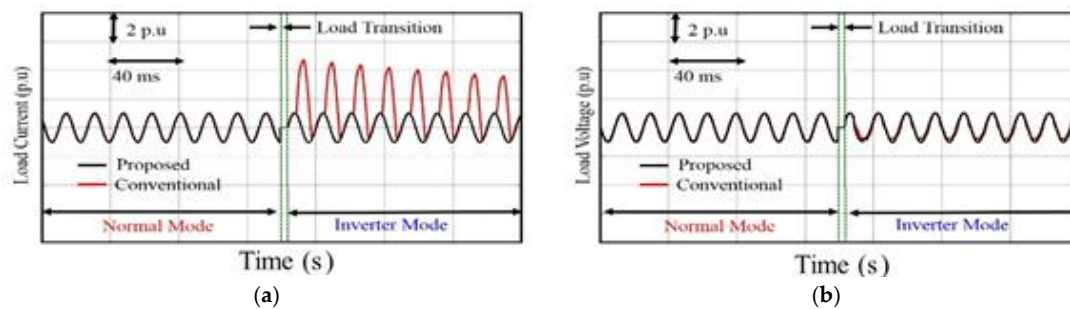


Figure 24. (a) Load current; and (b) load voltage for the conventional and proposed single-phase offline UPS topologies when the inverter voltage is injected at 360° .

3. Experimental Verification

To confirm the effectiveness of suggested single-phase offline UPS system, an experimental setup is built, and the parameters of the system are given in Table 4.

Table 4. System Parameters.

Parameter	Value
Utility/Grid	220 V, 60 Hz
DC Bus Voltage	365 V
Switching Frequency (f_s)	10 kHz
Transformer Ratings	500 VA, 220/220 V
Load Resistance (R_L)	90 Ω
Load Inductance (L_L)	10 mH
Filter Inductance (L_f)	0.265 mH
Filter Inductance (C_f)	10 μ F

The experimental set up of the proposed topology shown in Figure 25, consists of hardware, software, and firmware. The hardware consists of the control components, the power components, and an RL load. The control components are a DSP controller 320F28335 from Texas Instruments, and the interface, including ADC and DAC to facilitate the DSP controller connection with external hardware. The power component mainly consists of inverter power switches, a DC bus bar, and a heatsink. Power IGBTs from Semikon International SKM75GB128D are used as power switches for the inverter. The firmware is the control strategy that has already been discussed. The software component consists of the programming of the DSP controller according to the control algorithm to achieve the desired results. C language is used for programming the TMS320F28335 for the proposed UPS system topology. The performance of the controller of the proposed UPS system is not deteriorated by any of the switching or loading conditions and the currents are controlled perfectly as discussed in the previous section. Therefore, experimental results for only one case are provided.

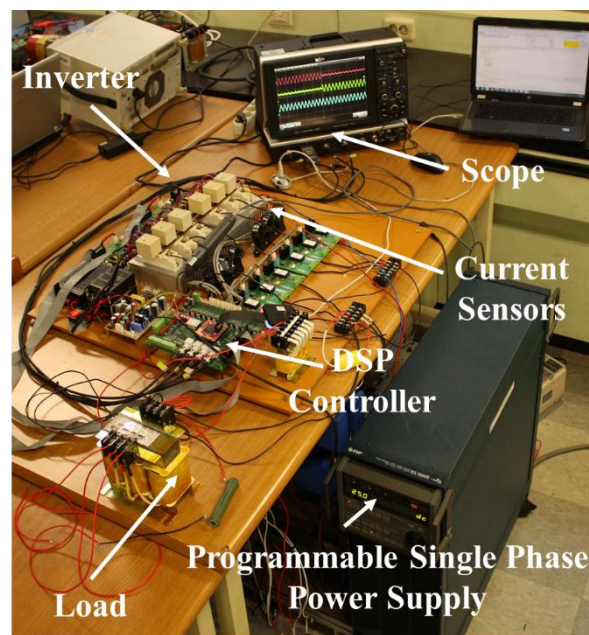


Figure 25. Experimental setup of the proposed single-phase offline UPS system.

The performance of the proposed single-phase offline UPS system was investigated during the changeover of load from the utility to the inverter, which takes 4 ms. Figure 26 shows the experimental waveform under such a condition. From the experimental result it is clear that the chance of the occurrence of inrush current during the transition of load is eliminated. To investigate the performance of the proposed offline UPS system while powering a load other than the motor or an RL loads, experiments have been performed using a transformer-coupled uncontrolled rectifier. The output of the rectifier is connected with a resistive element. From the implemented investigation, it is found that the performance of the proposed UPS system is not affected at any stage irrespective of the nature of load. Figure 27 shows the experimental results for the load and the rectifier output currents during inverter mode. The load current (I_{Load}) is measured at the primary of the load transformer. However, the rectifier output current is measured at the output of the rectifier connected to the resistor. It should be noted that the load current in the proposed UPS topology is dependent upon the current regulation capability of the current regulator. Therefore, any of the suitable current regulation schemes can be adopted according to the load characteristics.

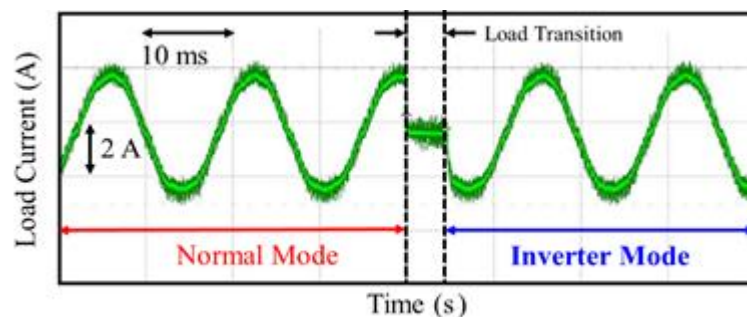


Figure 26. Experimental waveform of load current (I_{Load}) using proposed single-phase offline UPS system during the inverter operating mode.

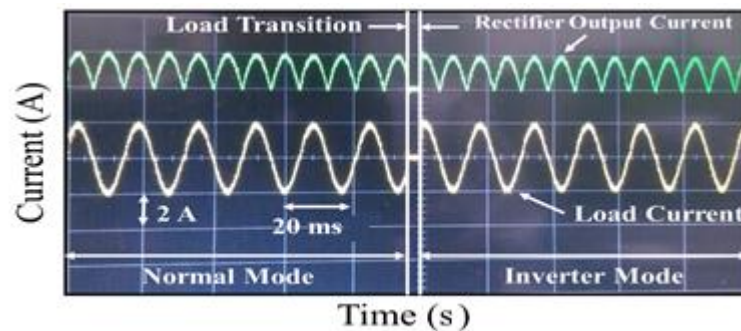


Figure 27. Experimental waveform of load current (I_{Load}), and rectifier output current for the proposed single-phase offline UPS system while powering a transformer-coupled uncontrolled rectifier load during inverter mode.

4. Conclusions

The problems related with the generation of inrush current when using a single-phase offline UPS system while powering a load transformer, have been discussed in this paper. It is demonstrated that by using a current regulated inverter at the place of the typical PWM voltage source inverter for a single-phase offline UPS system, the phenomenon of inrush current can be eliminated. Performance of the conventional and proposed UPS topologies were investigated and then compared. Furthermore, since the proposed topology is based on current regulation algorithm, which is ideally suitable for RL and motor loads, hence it offers relatively better performance than the conventional offline UPS system while dealing with non-linear loads. The proposed UPS system is also validated by experiment.

Acknowledgments: This research was jointly supported by the “BK21PLUS program” through the National Research Foundation of Korea funded by the Ministry of Education and the “Human Resources Program” in Energy Technology of the Korea Institute of Energy Technology Evaluation and Planning (KETEP), granted financial resource from the Ministry of Trade, Industry and Energy, Republic of Korea. (20154030200730).

Author Contributions: Syed Sabir Hussain Bukhari proposed the idea, implemented it by simulations and wrote the manuscript. Shahid Atiq performed the experiment and Byung-il Kwon supervised the research throughout.

Conflicts of Interest: The authors declare no conflict of interest.

References

1. Chen, Y.-H.; Cheng, P.-T. An Inrush Current Mitigation Technique for the Line-Interactive Uninterruptible Power Supply Systems. *IEEE Trans. Ind. Appl.* **2010**, *46*, 1498–1508.
2. Bukhari, S.S.H.; Lipo, T.A.; Kwon, B.-I. An inrush current reduction technique for the line-interactive uninterruptible power supply systems. In Proceedings of the 39th Annual Conference of the IEEE Industrial Electronics Society (IECON-2013), Vienna, Austria, 10–13 November 2013; pp. 430–434.
3. Bekiarov, S.B.; Emadi, A. Uninterruptible power supplies: Classification, operation, dynamics, and control. In Proceedings of the 17th Annual IEEE Applied Power Electronics Conference and Exposition (APEC), Dallas, TX, USA, 10–14 March 2002; pp. 597–604.
4. Bukhari, S.S.H.; Lipo, T.A.; Kwon, B.-I. An on-line UPS system that eliminates the inrush current phenomenon while feeding multiple load transformers. In Proceedings of the 9th International Conference on Power Electronics and ECCE Asia (ICPE-ECCE Asia), Seoul, Korea, 1–5 June 2015; pp. 385–390.
5. Muñoz-Cruzado-Alba, J.; Villegas-Núñez, J.; Vite-Frías, J.A.; Carrasco Solís, J.M. A New Fast Peak Current Controller for Transient Voltage Faults for Power Converters. *Energies* **2016**, *9*, 1.
6. Yeh, C.-C.; Manjrekar, M.D. A Reconfigurable Uninterruptible Power Supply System for Multiple Power Quality Applications. *IEEE Trans. Power Electron.* **2007**, *22*, 1361–1372. [[CrossRef](#)]
7. Kim, H.S.; Ji, J.-K.; Kim, J.-H.; Sul, S.-K.; Kim, K.-H. Novel topology of a line interactive UPS using PQR instantaneous power theory. In Proceedings of the 39th IEEE IAS Annual Meeting in Industry Applications Conference, Washington, DC, USA, 3–7 October 2004; pp. 2232–2238.

8. Kwon, B.-H.; Choi, J.-H.; Kim, T.-W. Improved single-phase line-interactive UPS. *IEEE Trans. Ind. Electron.* **2001**, *48*, 804–811.
9. Mokhtari, H.; Iravani, M.R.; Dewan, S.B. Transient behavior of load transformer during subcycle bus transfer. *IEEE Trans. Power Deliv.* **2003**, *18*, 1342–1349.
10. Steurer, M.; Frohlich, K. The impact of inrush currents on the mechanical stress of high voltage power transformer coils. *IEEE Trans. Power Deliv.* **2002**, *17*, 155–160.
11. Turner, R.A.; Smith, K.S. Transformer inrush currents. *IEEE Ind. Appl. Mag.* **2010**, *16*, 14–19. [[CrossRef](#)]
12. Li, Y.; Vilathgamuwa, D.M.; Loh, P.C. Microgrid power quality enhancement using a three-phase four-wire grid-interfacing compensator. *IEEE Trans. Ind. Appl.* **2005**, *41*, 1707–1719.
13. Lee, W.-C.; Lee, T.-K.; Hyun, D.-S. A three-phase parallel active power filter operating with PCC voltage compensation with consideration for an unbalanced load. *IEEE Tran. Power Electron.* **2002**, *17*, 807–814.
14. Chen, Y.-H.; Lin, C.-Y.; Chen, J.-M.; Cheng, P.-T. An Inrush Mitigation Technique of Load Transformers for the Series Voltage Sag Compensator. *IEEE Trans. Power Electron.* **2010**, *25*, 2211–2221. [[CrossRef](#)]
15. Zaltsman, V. Inrush current control for equipment powered by UPSs. In Proceedings of the INTELEC, Florence, Italy, 15–18 October 1989; Volume 2, pp. 19.4/1–19.4/7.
16. Jamali, M.; Mirzaie, M.; Gholamian, S.A. Calculation and Analysis of Transformer Inrush Current Based on Parameters of Transformer and Operating Conditions. *Electron. Electr. Eng.* **2011**, *3*, 17–20.
17. Loncarski, J.; Leijon, M.; Srndovic, M.; Rossi, C.; Grandi, G. Comparison of Output Current Ripple in Single and Dual Three-Phase Inverters for Electric Vehicle Motor Drives. *Energies* **2015**, *8*, 3832–3848.
18. Bukhari, S.S.H.; Kwon, B.-I.; Lipo, T.A. Unsymmetrical fault correction for sensitive loads utilizing a current regulated inverter. In Proceedings of the 29th Annual IEEE Applied Power Electronics Conference and Exposition (APEC), Fort Worth, TX, USA, 16–20 March 2014; pp. 366–370.
19. Kong, W.Y.; Holmes, D.G.; McGrath, B.P. Improved Stationary Frame AC Current Regulation using Feedforward Compensation of the Load EMF. In Proceedings of the 24th Annual IEEE Applied Power Electronics Conference and Exposition (APEC), Washington, DC, USA, 15–19 February 2009; pp. 145–151.
20. Holmes, D.G.; Lipo, T.A.; McGrath, B.P.; Kong, W.Y. Optimized Design of Stationary Frame Three Phase AC Current Regulators. *IEEE Trans. Power Electron.* **2009**, *24*, 2417–2426.
21. Dou, X.; Yang, K.; Quan, X.; Hu, Q.; Wu, Z.; Zhao, B.; Li, P.; Zhang, S.; Jiao, Y. An Optimal PR Control Strategy with Load Current Observer for a Three-Phase Voltage Source Inverter. *Energies* **2015**, *8*, 7542–7562.
22. Zhang, Y.; Li, M.; Kang, Y. PID Controller Design for UPS Three-Phase Inverters Considering Magnetic Coupling. *Energies* **2014**, *7*, 8036–8055.
23. Franklin, G.F.; Powell, J.D.; Workman, M.L. *Digital Control of Dynamic Systems*, 3rd ed.; Addison-Wesley: Menlo Park, CA, USA, 1998.
24. Yacamini, R.; Abu-Nasser, A. The calculation of inrush current in three-phase transformers. *IEE Proc. Electr. Power Appl.* **1986**, *133*, 31–40.
25. Bukhari, S.S.H.; Atiq, S.; Lipo, T.A.; Kwon, B.-I. A Cost-Effective, Single-Phase Line-Interactive UPS system that Eliminates Inrush Current Phenomenon for Transformer-Coupled Loads. *J. Electr. Eng. Technol. (JEET)* **2016**, *11*, 709–718.
26. Bukhari, S.S.H.; Atiq, S.; Lipo, T.A.; Kwon, B.-I. Line-Interactive UPS system that Eliminates Inrush Current Phenomenon. *Electr. Power Compon. Syst.* **2016**, in press.

